Check for updates

Antibacterial Activity of Two Metabolites Isolated From Endophytic Bacteria *Bacillus velezensis* Ea73 in *Ageratina adenophora*

Zhihua Ren [1†], Lei Xie [1†], Samuel Kumi Okyere [1†], Juan Wen [1], Yinan Ran [1], Xiang Nong [2] and Yanchun Hu [1*]

[1] Key Laboratory of Animal Disease and Human Health of Sichuan Province, College of Veterinary Medicine, Sichuan Agricultural University, Yaan, China, [2] College of Life Science, Leshan Normal University, Leshan, China

Ageratina adenophora, as an invasive and poisonous weed, seriously affects the ecological diversity and development of animal husbandry. Weed management practitioners have reported that it is very difficult to control *A. adenophora* invasion. In recent years, many researchers have focused on harnessing the endophytes of the plant as a useful resource for the development of pharmacological products for human and animal use. This study was performed to identify endophytes with antibacterial properties from *A. adenophora*. Agar well diffusion method and 16S rRNA gene sequencing technique were used to screen and identify endophytes with antibacterial activity. The response surface methodology and prep- high-performance liquid chromatography were used to determine the optimizing fermentation conditions and isolate secondary metabolites, respectively. UV-visible spectroscopy, infrared spectroscopy, nuclear magnetic resonance, and high-resolution mass spectrum were used to determine the structures of the isolated metabolites. From the experiment, we isolated a strain of *Bacillus velezensis* Ea73 (GenBank no. MZ540895) with broad-spectrum antibacterial activity. We also observed that the zone of inhibition of *B. velezensis* Ea73 against *Staphylococcus aureus* was the largest when fermentation broth contained 6.55 g/L yeast extract, 6.61 g/L peptone, 20.00 g/L NaCl at broth conditions of 7.95 pH, 51.04 h harvest time, and a temperature of 27.97°C. Two antibacterial peptides, Cyclo (*L*-Pro-*L*-Val) and Cyclo (*L*-Leu-*L*-Pro), were successfully extracted from *B. velezensis* Ea73. These two peptides exhibited mild inhibition against *S. aureus* and *Escherichia coli*. Therefore, we isolated *B. velezensis* Ea73 with antibacterial activity from *A. adenophora*. Hence, its metabolites, Cyclo (*L*-Pro-*L*-Val) and Cyclo (*L*-Leu-*L*-Pro), could further be developed as a substitute for human and animal antibiotics.

Keywords: *Ageratina adenophora*, endophytes, *Bacillus velezensis* Ea73, secondary metabolites, antibacterial compound

INTRODUCTION

The abuse of antibiotics over the past few years has led to the emergence of drug-resistant pathogens, resulting in serious health complications in humans and animals (Ding et al., 2016; Chernov et al., 2019). Due to this setback, the search for new and effective antibiotics from natural sources has become an alternative strategy over the past few decades. The main sources of natural antibiotics are animals and plants. However, due to challenges, such as the bulky nature, slow-growing, endangered species, and high cost, associated with the use of animal and plant resources in excessive development of antibiotics, microorganisms may serve as the best alternative for harnessing pharmacological bioactive compounds for the development of drugs for both human and animal use because they are easy to handle and cheap to produce (Wen et al., 2022).

Studies have showed that endophytes are ubiquitous in all kinds of plants and are rich in species (Hallmann et al., 2011). They produce many secondary metabolites with various biological activities such as antibacterial and antitumor. They also enhance plant resistance to diseases and insect pests (Strobel et al., 2004; Tosi et al., 2021). Therefore, endophytes are a perfect alternative for the identification and production of antibacterial compounds.

The invasive nature of *Ageratina adenophora* (Spreng). R. M. King et H. Rob. is attributed to the plant's strong adaptability and breeding ability (Kong et al., 2017). The plant secretes allelochemicals that inhibit the growth of other plants, thereby forming a single dominant community and eventually destroying the ecological structure (Mcgeoch et al., 2010). *A. adenophora* has caused serious health conditions in animals, which has resulted in huge economic losses in the agriculture, forestry, and animal husbandry sectors (He et al., 2016; Tripathi et al., 2018; Okyere et al., 2020, 2021a; Cui et al., 2021; Ren et al., 2021a,b). Over the past few years, various control measures and strategies were developed to reduce the spread of *A. adenophora*; however, these programs have not yielded good results, and therefore, the utilization of the plant's resources (such as plant parts, extracts, metabolites, and endophytes) for the benefit of mankind has been the research direction over the past few years (Wan et al., 2010; Okyere et al., 2021b, 2022). *A. adenophora* has shown many biological activities such as insecticidal (Samuel et al., 2014), antibacterial (Yao et al., 2019), antitumor (Liao et al., 2014), antivirus (Jin et al., 2014), and antioxidation (Zhang et al., 2013).

Microorganisms have a complex symbiotic relationship with plants (Trivedi et al., 2020). Numerous studies have reported that endophytes produce similar secondary metabolites just as their host plant (Tanapichatsakul et al., 2018, 2019). Therefore, we hypothesized that endophytes from *A. adenophora* may possess antimicrobial activity, thus requiring investigation.

Ageratina adenophora endophytes have showed various biological activities. For example, a study by Jiang (2010) revealed that *Bacillus megaterium* isolated from *A. adenophora* showed growth-promoting activity (Jiang, 2010). Another study also reported that *Arbuscular mycorrhizal* fungi from *A. adenophora* had heavy metal repair activity (Kang, 2010). Fungi endophyte (*Coniochaeta* sp. F-8) also showed antioxidant

activity (Fu et al., 2021). However, studies on the isolation of antibacterial endophytes and their metabolites from *A. adenophora* are limited; therefore, this study was performed to isolate antibacterial bacteria endophytes and their major metabolites from *A. adenophora*. This study will help us identify bacterial endophytes with antibacterial properties from *A. adenophora* to help in the development of probiotics and antibacterial drugs.

MATERIALS AND METHODS

Plant Sample, Chemicals, and Reagents

Leaves, roots, stems, and flowers of *A. adenophora* were collected from Wangsuo Village, Cangzhou Street, Dechang County, Liangshan Yi Autonomous Prefecture, Sichuan Province ($102°15'20''$ E and $27°20'11''$ N; elevation $=2,152$ m). The samples were confirmed as *A. adenophora* by Prof. Chao Hu, Department of Botany, Sichuan Agricultural University. Culture media were purchased from Qingdao Hope Bio-Technology Co., Ltd., Qingdao, China. *Escherichia coli* ATCC 35218, *Salmonella tropina* H9812, *Pseudomonas aeruginosa* ATCC 27853, *Klebsiella pneumoniae* CMCC 46109, and *Staphylococcus aureus* CPCC 140594 were obtained from the College of Veterinary Medicine (Professor Xueqin Ni's lab), Sichuan Agricultural University, China.

Isolation of Endophytic Bacteria

The fresh root, stem, leaf, and flower tissues of *A. adenophora* were washed with sterile water, then soaked in 3% NaClO for 3 min, 0.1% HgCl$_2$ for 3 min, 75% ethanol for 3 min. Afterward, they were washed with sterile water five times and dried with sterile filter paper (Liang et al., 2009). The tissues were cut into 1 cm × 1 cm pieces with a sterile knife and plated on LB agar medium. After 2–3 days of culture in an incubator at 30 ± 2°C, the growing colonies were isolated and purified by cross-streaking on LB agar plates until pure strains were obtained.

Screening of Antibacterial Activity

The indicator microorganisms used for antimicrobial activity assays throughout this study were *E. coli* ATCC 35218, *S. tropina* H9812, *P. aeruginosa* ATCC 27853, *K. pneumoniae* CMCC 46109, and *S. aureus* CPCC 140594. The indicator microorganisms were inoculated in LB broth and cultured at 37 ± 2°C in a 150 r/min shaker until it reached a logarithmic phase of about 14 h. After centrifugation at 4,000 r/min, the bacterial precipitates were collected and adjusted to a concentration of 1 × 10^6 CFU/ml with sterile normal saline to form the pathogen suspension. The endophytic bacteria with antibacterial activity were screened by well diffusion method (du Toit and Rautenbach, 2000). Then, 60 μl sterile fermentation liquid was loaded into each well. Sterile normal saline was used as blank control. After incubation at 30 ± 2°C for 24 h, the inhibitory zone diameter (mm) was measured using a Vernier caliper. The experiment was repeated three times.

Identification of Endophytic Bacteria
Morphological Identification

Strain Ea73 was inoculated on LB agar and cultured at $37 \pm 2^{\circ}C$ for 24 h. Morphological characteristics of the colony were observed using microscopy, and Gram staining was performed using Gram Stain Kit (Haibo Biotechnology Co., Ltd., Qingdao).

Molecular Identification

Endophytic bacterial isolate that exhibited antimicrobial activity was identified based on 16S rRNA sequence. The primers used to amplify the 16S rRNA sequence of the strain were 27F: 5′-AGAGTTTGATCCTGGCTCAG-3′ and 1492R: 5′-GCTTAC CTTGTTACGACTT-3′. PCR amplification system (25 μl): template DNA 2 μl, 2× Taq PCR Master Mix 12.5 μl, primer 27F (10 μmol/L) 1 μl, primer 1492R (10 μmol/l) 1 μl, DD H_2O 8.5 μl. PCR reaction conditions: 95°C for 10 min. There were 35 cycles at 95°C for 1 min, 56°C for 30 s, 72°C for 2 min, 72°C for 10 min (Amin et al., 2020). The amplified products were sent to Youkang Biological (Chengdu) Co., Ltd. for sequencing and splicing. Consensus sequences were analyzed using BLASTN available from the National Center of Biotechnology Information (NCBI) website. Identity of endophytic bacteria was based on the percentage of homology to sequences available in the database. Further, MEGA 6 software was used to construct the phylogenetic trees using neighbor-joining and maximum parsimony method based on bootstrap values (1,000 replications) (Dereeper et al., 2010). The 16S rRNA gene sequence (1,497 bp) was submitted to NCBI GenBank with accession id MZ540895.

Fermentation Condition Optimization
Optimization of Medium Composition

Taking the inhibitory zone diameter for *S. aureus* as an indicator, single-factor test was used to select the best carbon source, nitrogen source, inorganic salt, and their optimal concentration. The procedures are as follows.

Optimization of Carbon Source

The carbon source in LB medium was replaced with yeast extract, glucose, soluble starch, sucrose, and mannitol, and the best carbon source was selected under the same conditions. The optimal carbon source concentration was determined by adding different concentration gradients of 2.0, 5.0, 10.0, 15.0, 20.0, and 25.0 g/L, respectively.

Optimization of Nitrogen Sources

The nitrogen source in LB medium was replaced with tryptone, peptone, beef extract, $(NH_4)_2SO_4$, and urea, and the best nitrogen source was selected under the same conditions. The optimal nitrogen source concentration was determined by adding different concentration gradients of 5.0, 10.0, 15.0, 20.0, 25.0, and 30.0 g/L, respectively.

Optimization of Inorganic Sources

The inorganic salt in LB medium was replaced with NaCl, $MgSO_4$, KCl, $CuSO_4$, and $CaCl_2$, and the best inorganic salt source was selected under the same conditions. The optimal inorganic salt concentration was determined by adding different concentration gradients of 5.0, 10.0, 15.0, 20.0, 25.0, and 30.0 g/L, respectively.

According to the single-factor results, a Box-Behnken central composite design principle with carbon source (A), nitrogen source (B), and inorganic salt (C) as independent variables, and inhibitory zone diameter as response value, was adopted for carrying out a three-factor and three-level response surface test design. The results were statistically analyzed using Design Expert 7.0 statistical software (Sun et al., 2009).

Optimization of Fermentation Parameters

Taking the inhibitory zone diameter for *S. aureus* as an indicator, single-factor test was used to select the best fermentation initial pH, temperature, and time of medium. The procedures were as follows.

Fermentation pH

On the basis of optimal medium composition, pH was adjusted to 4.0, 5.0, 6.0, 7.0, 8.0, 9.0, and 10.0, respectively, and fermentation at 30°C for 48 h, to determine the best initial pH.

Fermentation Temperature

On the basis of optimal medium composition, pH was adjusted to 7. Fermentation was conducted at 24, 27, 30, 33, 36, and 39°C for 48 h to determine the optimal fermentation temperature.

Fermentation Time

On the basis of optimal medium composition, pH was adjusted to 7 and temperature to 30°C. Fermentation time of 24, 48, 72, 96, and 120 h, respectively, was used to determine the best fermentation time.

According to single-factor results, a Box-Behnken central composite design principle with initial pH (A), temperature (B), and time (C) as independent variables, and the inhibitory zone diameter as the response value, was adopted. Design Expert 7.0 statistical software was used to analyze the experimental results, and the optimal fermentation parameters were obtained (Sun et al., 2009).

Isolation and Identification of Antibacterial Metabolites

Ea73 strain was activated and fermented under the optimum fermentation conditions. After the fermentation, the broth was broken by ultrasonic wave (40 Hz, 20 min), and the organic phase was collected by multiple extraction with ethyl acetate, and concentrated to dry at 45°C with rotary evaporator. The extractum was subjected to silica gel column chromatography with stepwise elution of chloroform:methanol (30:1, 20:1, 10:1, 6:1, 1:1; v/v). All eluted fractions were separately collected and concentrated using an evaporator. The fraction (20:1) was separated by gel filtration on Sephadex LH-20 column using running phase of 100% methanol. The eluted components were further purified by prep-high-performance liquid chromatography (HPLC) (Agilent 1260 series HPLC system):preparative reversed-phase column (10 μm, 250 mm × 20 mm), at a flow rate of 10 ml/min, methanol:H_2O (25: 75, v/v), and UV detection at 210 nm. The purity of the separated

compounds was further detected by HPLC (Agilent 1260 series HPLC system):C18 column (5 μm, 4.6 × 150 mm) at a flow rate of 1.0 ml/min, methanol-water (20–100% methanol in water over 8.0 min followed by 100% methanol to 13.0 min), and UV detection at 210 nm.

Structural Identification

The structures of the two compounds were characterized using UV, infrared (IR), nuclear magnetic resonance (NMR), and high-resolution mass spectrum (HRMS). UV-visible spectrophotometer (AOI Instrument Co. Ltd., A390, Shanghai, China) was used to measure the UV-Vis spectra of the systems in this work. The Fourier-transform infrared spectroscopy (FTIR) spectrum, obtained from a Fourier transform infrared spectrometer (FTIR-840OS, Shimadzu, Japan), was used to identify functional groups. The structure of the compounds was determined using NMR spectroscopy (Bruker DRX 500 NMR instrument, Bruker, Rheinstetten, Germany) equipped with a 2.5 mm microprobe. NMR spectrometer using $CDCl_3$ was deployed to measure ^1H and ^{13}C NMR. HRMS was performed on a Thermo Scientific Exactive Orbitrap LC-Mass Spectrometer with an electrospray ionization mode.

Antibacterial Assay

Minimum inhibitory concentration (MIC) evaluation of compounds (**1** and **2**) was carried out in a 96-well plate according to the standard microdilution method. *E. coli* and *S. aureus* were used for this assay. The sterilized 96-well plates were taken from the 1st to the 11th rows from left to right, and 100 μl of sterilized MH medium was loaded into each well. This was done in triplicate. Afterward, 100 μl of the tested compound in the adjusted concentration was loaded into the second well. Then, it was continuously diluted to the 11th well. Afterward, 100 μl of mixture in the 11th well was discarded. Finally, 25 μl of the tested strain suspension was added to make the final concentration of the compound 512, 256, 128, 64, 32, 16, 8, 4, 2, and 1 μg/ml. Both blank control and positive control had no tested compound. Using the obvious growth of the negative control wells as an indicator, the sterile growth and non-turbidity holes in the 96-well plate were considered the MIC holes (Jeong et al., 2017).

Statistical Analysis

Statistical analysis of the data collected (from various independent experiments) was performed using SPSS 22 Statistical Analysis Software (SPSS Inc., Chicago, IL, USA). All experimental results are presented as mean ± SD, and statistical significance was determined by one-way analysis of variance (ANOVA) followed by Tukey's test. The values were significantly different at $p < 0.05$.

RESULTS

Screening of Strain Ea73

Out of the 95 endophytic bacteria that were isolated from the roots, stems, leaves, and flowers of *A. adenophora,* only 21 strains showed antibacterial activity after screening using the well

TABLE 1 | Growth inhibitory zone diameter (mm) of pathogens with Ea73 bacteria isolated from *Ageratina adenophora*.

Pathogens	Inhibitory zone diameter (mm)
Escherichia coli ATCC 35218	10.57 ± 0.18
Salmonella tropina H9812	9.69 ± 0.17
Pseudomonas aeruginosa ATCC 27853	13.72 ± 0.36
Klebsiella pneumoniae CMCC 46109	11.00 ± 0.09
Staphylococcus aureus CPCC 140594	32.16 ± 2.04

diffusion method. These 21 strains had inhibitory effect on one or more pathogenic bacteria. However, strain Ea73 had universal antibacterial activity against all the five tested pathogenic bacteria used in this study with *S. aureus* being the most inhibited pathogenic bacteria (**Table 1**). Strain Ea73 was submitted for preservation in the China Center for Typical Culture Collection (CCTCC) on September 6, 2021, preservation number CCTCC M 20211139.

## Identification of Endophytic Bacteria

Strain Ea73 was a short rod-shaped and Gram-positive bacteria. It also showed colony morphology characteristics of milky white, round or oval, opaque, rough surface, neat edges, and smooth myxoid colonies. The 16S rDNA sequence of strain Ea73 was analyzed using BLAST with a known nucleic acid sequence in GenBank. The results showed that strain Ea73 was similar to *Bacillus*. In addition, phylogenetic analysis results showed that the strain was in the same minimum branch as *Bacillus velezensis*, whose accession number was NR116240 (**Figure 1**). Therefore, strain Ea73 was identified as *B. velezensis* and named as *B. velezensis* Ea73. The gene sequence was submitted to GenBank with accessory number MZ540895.

Fermentation Condition Optimization
Optimizing the Medium Composition by Response Surface Methodology

Using a single-factor experiment, we observed that the best carbon source was yeast extract (5.0 g/L), nitrogen source was peptone (10.0 g/L), and the best inorganic salt was NaCl (15.0 g/L) (**Figure 2**). A response surface design was further applied when the optimal region for running the process was being identified. Taking carbon source (A), nitrogen source (B), and inorganic salt (C) as independent variables and the inhibitory zone diameter as response values, a three-factor and three-level response surface experiment was designed (**Table 2**).

The Design Expert software was used to perform quadratic multiple regression fitting for the experimental data (**Table 3**). The quadratic multiple regression model equation of R for each factor was represented as R = 34.14 + 0.60 A-0.49 B + 0.016 C + 0.18 AB-0.20 AC-0.83 BC-1.00 A^2-0.96 B^2 + 0.11 C^2. The regression model was significant ($p < 0.05$), indicating that the experimental model was statistically significant. According to the *p*-value, the variables A, B, BC, A^2, and B^2 in the model had a significant effect on the inhibitory zone diameter ($p < 0.05$), indicating that there is no linear relationship between

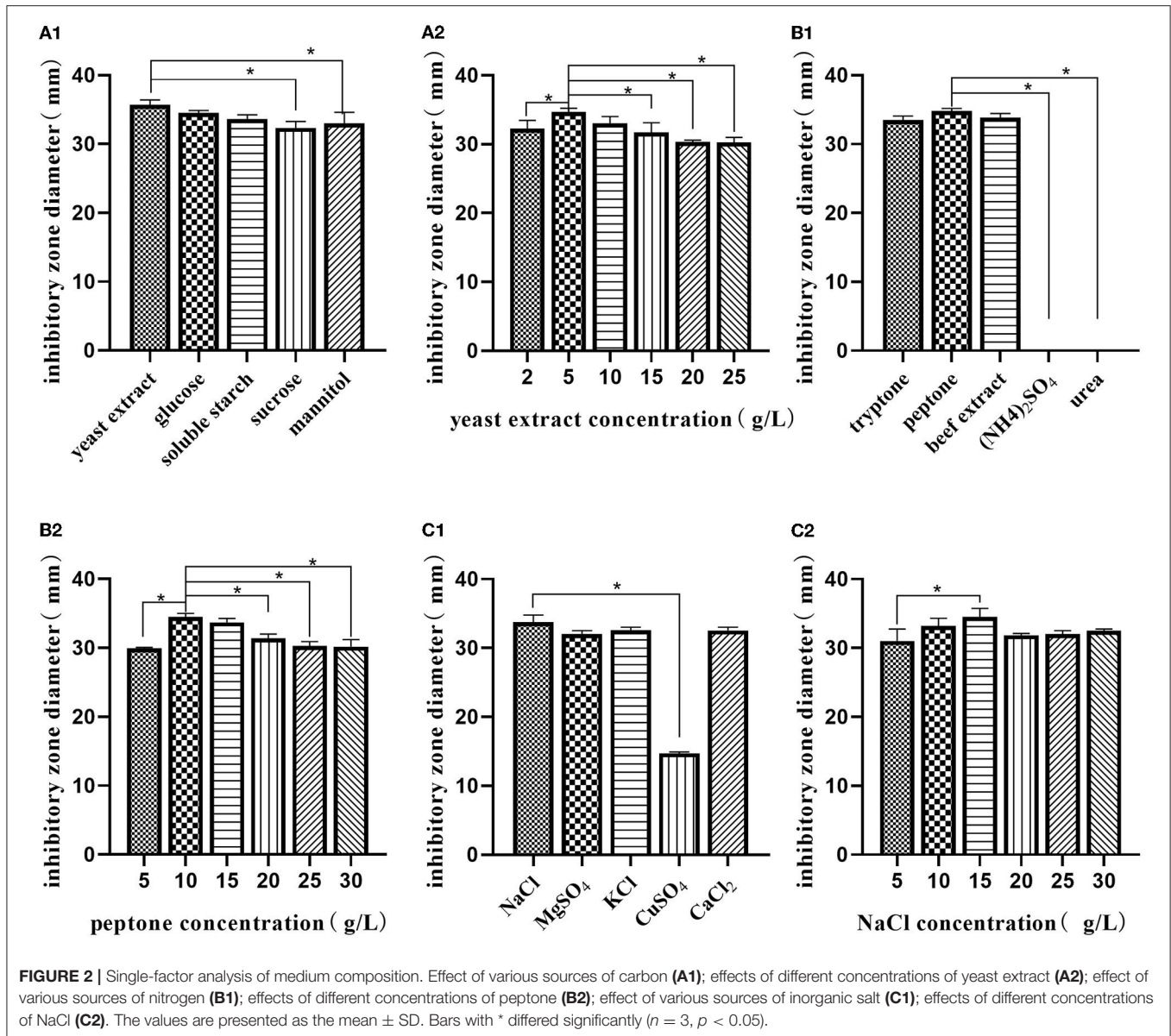**FIGURE 1 |** Phylogenetic tree of *Bacillus velezensis* strain Ea73.
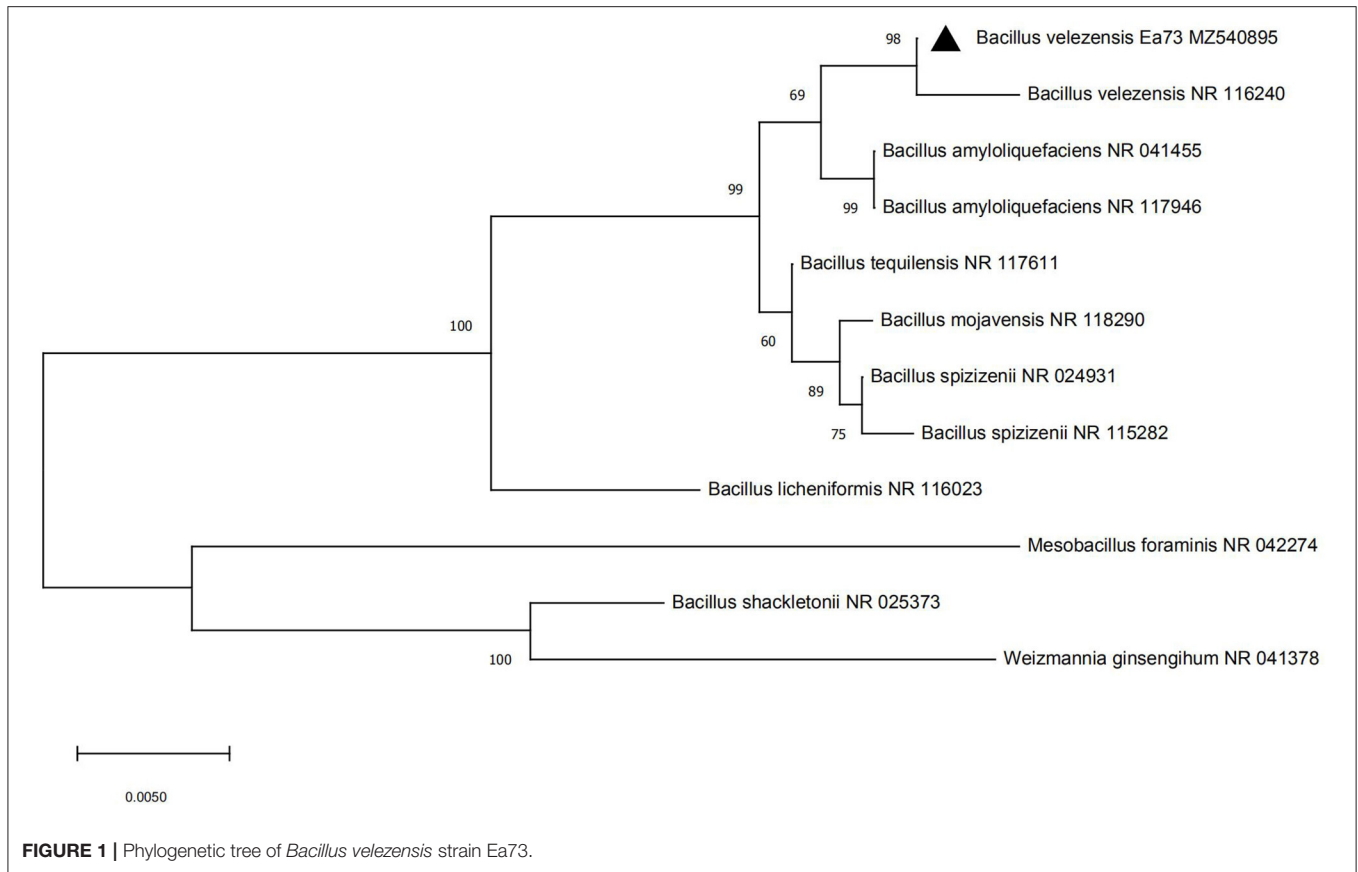
the experimental factors and the response value; however, the interaction of the primary term, quadratic term, and BC had a close relationship with the response value. Lack of fit was not significant ($p > 0.05$), indicating that the fitting degree of the experimental model was good, the selection of the model was reasonable, and the residual of the model may be a result of the random error in the experimental process. The correction determination coefficient $R^2_{Adj} = 0.7738$ of the model shows that 77.38% of the variation in the experiment was distributed in the factors of the equation, and the R^2-value is 0.9192, indicating that there is a good fit between the measured value and the predicted value of inhibitory zone diameter. The model can be used to predict the actual situation of inhibitory zone diameter.

Figure 3 displays the response surface curves as interaction between the yeast extract, peptone, and NaCl on inhibitory zone diameter. It directly shows the response over a region of independent variables and the relationship between experimental levels of each factor. Each figure demonstrates the effect of two factors while the other factor was fixed at zero level. **Figure 3A** represents the effect of yeast extract concentration and peptone concentration on inhibitory zone diameter at a fixed NaCl concentration of 15.0 g/L. The results showed that the maximum response value was obtained when the yeast extract concentration was 7.0 g/L and peptone concentration was 9.0 g/L. The effect of yeast extract concentration and NaCl concentration on the inhibitory zone diameter at a fixed peptone concentration of

10.0 g/L is shown in **Figure 3B**. Decreasing the yeast extract concentration led to an increase in the inhibitory zone diameter, irrespective of the NaCl concentration. The response value that reached its highest point at yeast extract concentration was 7.0 g/L. **Figure 3C** shows the effect of peptone concentration and NaCl concentration on the inhibitory zone diameter at a fixed yeast extract concentration of 5.0 g/L. Increasing the concentration of NaCl resulted in an increase in the response surface. The response value reached its highest point at 7.0 g/L of peptone concentration and 20.0 g/L of NaCl concentration. Therefore, from the surface response graphs and the regression analysis of the equation, it was concluded that the optimal conditions for inhibitory zone diameter were located in the region where yeast extract, peptone, and NaCl concentration were 6.55, 6.61, and 20.00 g/L, respectively.

Optimizing the Fermentation Parameters by Response Surface Methodology

The optimal initial pH, temperature, and time were selected using the composition of media in the "Optimizing the medium composition by response surface methodology" section. Using single-factor screening, we observed that the initial pH, temperature, and time of the center were 8, 27°C, and 48 h, respectively (**Figure 4**). Taking initial pH (A), temperature (B), and time (C) as independent variables and inhibitory zone

FIGURE 2 | Single-factor analysis of medium composition. Effect of various sources of carbon **(A1)**; effects of different concentrations of yeast extract **(A2)**; effect of various sources of nitrogen **(B1)**; effects of different concentrations of peptone **(B2)**; effect of various sources of inorganic salt **(C1)**; effects of different concentrations of NaCl **(C2)**. The values are presented as the mean ± SD. Bars with * differed significantly ($n = 3$, $p < 0.05$).

diameter as response values, a three-factor and three-level response surface experiment was designed (**Table 4**).

The Design Expert software was used to perform quadratic multiple regression fitting for the experimental data (**Table 5**). The quadratic multiple regression model equation of R for each factor was represented as $R = 40.47 - 0.010\,A + 1.43\,B + 1.02\,C - 0.29\,AB + (5.000\text{E-}003)\,AC - 0.72\,BC - 1.04\,A^2 - 2.10\,B^2 - 3.11\,C^2$. The regression model was significant ($p < 0.05$), and the variables B, C, B^2, and C^2 in the model had a significant effect on the inhibitory zone diameter ($p < 0.05$). Lack of fit was not significant ($p > 0.05$). The correction determination coefficient was $R^2_{Adj} = 0.7221$ and the R^2-value was 0.9192, indicating that the model could be used to predict the actual situation of inhibitory zone diameter.

Figure 5 displays the response surface curves from the interaction among initial pH, temperature, and time on

inhibitory zone diameter. **Figure 5A** represents the effect of original pH and temperature on zone of inhibition at a fixed time of 48 h. The results showed that the maximum response value was obtained when pH was 8 and temperature was 28°C. **Figure 5B** also represents the effect of original pH and time on inhibitory zone diameter at a fixed temperature of 27°C. The result showed that the maximum response value was obtained when the original pH was 8 and time was 51 h. **Figure 5C** represents the effect of original pH and time on inhibitory zone diameter at a fixed pH of 8. We observed that the maximum response value was obtained when the temperature was 28°C and time was 51 h. Therefore, from the surface response graphs and the regression analysis of the equation, it was concluded that the optimal conditions for inhibitory zone diameter were located in the region where initial pH, temperature, and time were 7.95, 27.97°C, and 51.04 h, respectively.

TABLE 2 | Design and experimental results of Box–Behnken design (medium composition).

Run	A (g/L)	B (g/L)	C (g/L)	Response (mm)
1	2	5	15	32.14
2	10	5	15	33.39
3	2	15	15	30.58
4	10	15	15	32.64
5	2	10	10	32.32
6	10	10	10	33.61
7	2	10	20	33.45
8	10	10	20	33.65
9	5	5	10	32.91
10	5	15	10	33.68
11	5	5	20	34.15
12	5	15	20	31.60
13	5	10	15	34.12
14	5	10	15	33.93
15	5	10	15	33.73

TABLE 3 | ANOVA results of the quadratic model (medium composition).

Source	Sum of squares	df	Mean square	F-Value	p-Value, Probability > F
Model	13.50	9	1.50	6.32	0.0281
A	2.88	1	2.88	12.14	0.0176
B	1.85	1	1.85	7.81	0.0382
C	1.947E-003	1	1.947E-003	8.202E-003	0.9314
AB	0.13	1	0.13	0.57	0.4861
AC	0.17	1	0.17	0.72	0.4353
BC	2.76	1	2.76	11.61	0.0191
A2	3.13	1	3.13	13.17	0.0151
B2	3.37	1	3.37	14.21	0.0130
C2	0.048	1	0.048	0.20	0.6713
Residual	1.19	5	0.24		
Lack of fit	1.11	3	0.37	9.73	0.0946
Pure error	0.076	2	0.038		
Cor total	14.69	14			

In conclusion, the results showed that the yield of antibacterial metabolites reached the maximum when the yeast extract was 6.55 g/L, peptone was 6.61 g/L, NaCl was 20.00 g/L, initial pH was 7.95, time was 51.04 h, and temperature was 27.97°C. Under these conditions, the inhibitory zone diameter of Ea73 fermentation broth against *S. aureus* reached 40.76 mm.

Isolation and Identification of Antibacterial Metabolites From *B. velezensis* Ea73

Using ethyl acetate, 4 L of fermentation broth was extracted, concentrated, and dried to obtain about 1 mg crude extract. The crude extract was further separated into five components (Fr_1-Fr_5) by silica gel column chromatography. After antibacterial activity and HPLC detection, the Fr_4 components at 20:1

(chloroform/methanol) elution concentration were further separated into Fr_{4-1} and Fr_{4-2} by Sephadex LH-20 column. The two components were purified by the prep-HPLC, respectively. Compound **1** (3.4 mg) was obtained by collecting components at the retention time 4.19 min of Fr_{4-1}. Compound **2** (5 mg) was obtained by collecting components at the retention time 4.58 min of Fr_{4-2}. The purity of the two compounds was detected by HPLC. The purity of the compounds recorded was more than 98%, according to the peak area from the chromatogram (**Figure 6**).
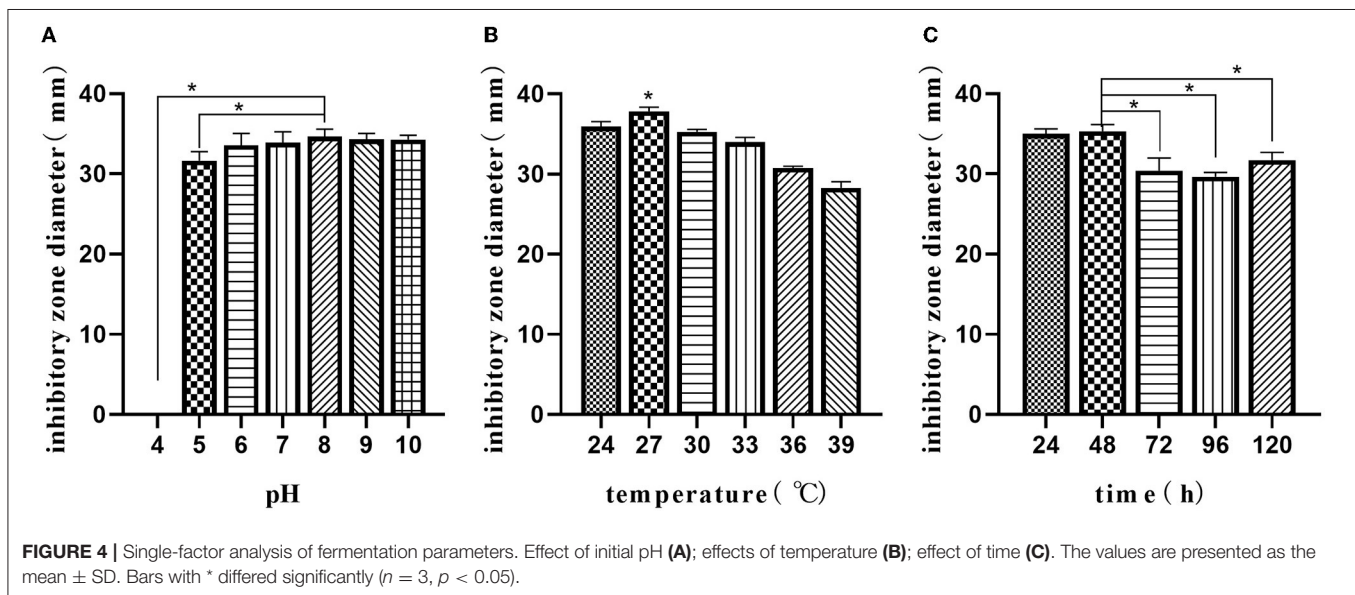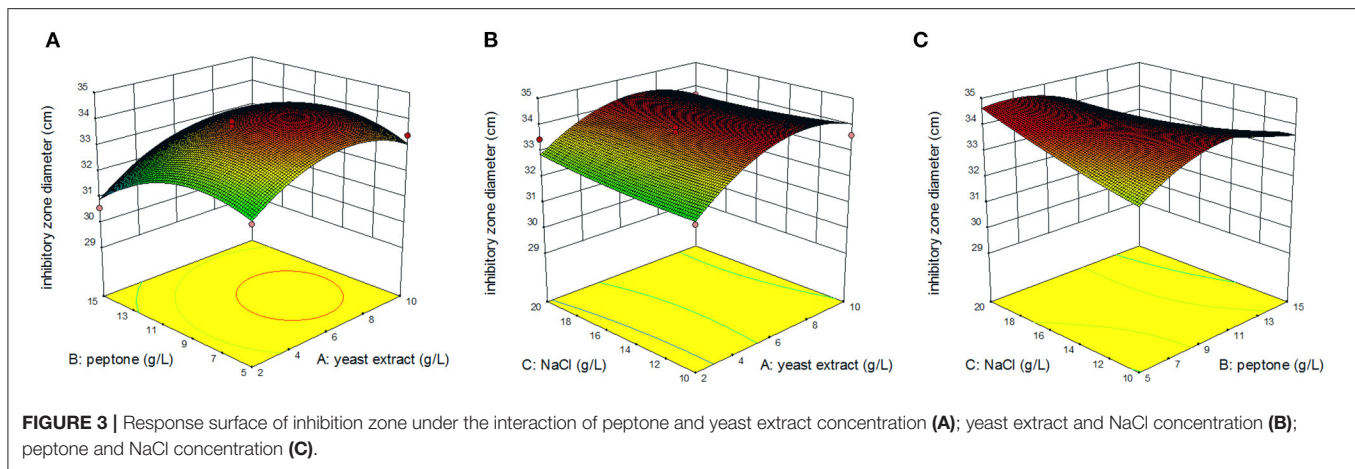
Characterization of Compound

Compound **1** was isolated as a white powder. The molecular formula of compound **1** was established as $C_{10}H_{16}N_2O_2$ by HRESIMS at m/z 197.1284 $[M+H]^+$ (calculated for $C_{10}H_{16}N_2O_2$: 197.1282). The IR spectrum showed the characteristic absorption at 3,438 cm^{-1} and 1,656 cm^{-1}, suggestive of imino group and carbonyl group, respectively. In the UV spectrum, there was no obvious ultraviolet absorption. ^{1}H-NMR spectra showed that the active hydrogen signal in one amide was δ 6.07 (1H, s), and four hydrogen were between δ4.2 and 3.5, adjacent to the regions of nitrogen, in which 4.09–4.05 (m, 1H), and 3.95–3.90 (m, 1H) were simultaneously absorbed by carbonyl and nitrogen with a larger chemical shift; 3.67–3.59 (m, 1H), and 3.57–3.48 (m, 1H) were hydrogen on chiral carbon, and two double peaks near δ 1.0, 1.06 (d, J = 7.3 Hz, 3H), 0.90 (d, J = 6.8 Hz, 3H) belong to methyl hydrogen. ^{13}C NMR carbon spectrum and DEPT spectrum give 10 carbon signals, including 2 methyl signals δ 19.23, 16.07; 3 methylene signals δ 45.15, 28.54, 22.38; and 3 methylene signals δ 60.40, 58.83, 28.39. Among them, δ 170.08, 164.94 was the carbonyl peak, and δ 60–40 was the leading carbon of nitrogen (**Supplement Figure 1**, **Table 6**). By comparing the above information with the literature (Pedras et al., 2005), compound **1** was determined to be (3S,8aS)-3-propan-2-yl-2,3,6,7,8,8a-hexahydropyrrolo[1,2-a]pyrazine-1,4-dione, also known as Cyclo (*L*-Pro-*L*-Val) (**Figure 7A**).

Compound **2** was isolated as a white powder. The molecular formula of **2** was established as $C_{11}H_{18}N_2O_2$ by HRESIMS at m/z 211.1441 $[M + H]^+$ (calculated for $C_{11}H_{18}N_2O_2$: 211.1438). The IR spectrum showed characteristic absorption at 3,430 and 1,660 cm^{-1}, suggestive of imino group and carbonyl group, respectively. In the UV spectrum, there was no obvious ultraviolet absorption. The NMR spectrum of compound **2** was very similar to that of compound **1**, with one more methylene (δ38.64) (**Supplement Figure 2**, **Table 6**). Based on NMR data and literature analysis (Pedras et al., 2005), compound **2** was determined to be (3S,8aS)-3-(2-methylpropyl)-2,3,6,7,8,8a-hexahydropyrrolo[1,2-a]pyrazine-1,4-dione, also known as Cyclo (*L*-Leu-*L*-Pro) (**Figure 7B**).

Antibacterial Assay of Two Compounds

The MIC values of the two compounds were determined using a 96-well plate assay. Both compounds were found to have inhibitory effects on *E. coli* ATCC 35218 and *S. aureus* CPCC 140594. Cyclo (*L*-Pro-*L*-Val) showed the MIC values of 512 and 256 μg/ml for *E. coli* and *S. aureus*, respectively, whereas Cyclo

FIGURE 3 | Response surface of inhibition zone under the interaction of peptone and yeast extract concentration **(A)**; yeast extract and NaCl concentration **(B)**; peptone and NaCl concentration **(C)**.

FIGURE 4 | Single-factor analysis of fermentation parameters. Effect of initial pH **(A)**; effects of temperature **(B)**; effect of time **(C)**. The values are presented as the mean ± SD. Bars with * differed significantly ($n = 3$, $p < 0.05$).

(L-Leu-L-Pro) showed an MIC value of 512 µg/ml for both two pathogenic bacteria.

DISCUSSION

In this study, *B. velezensis* was successfully isolated from *A. adenophora*, and its fermentation broth had general antibacterial activity against *E. coli*, *Salmonella*, *P. aeruginosa*, *K. pneumonia,* and *S. aureus*. *B. velezensis* have similar molecular characteristics to *Bacillus amyloliquefaciens* and *Bacillus methylotrophicus* (Rabbee et al., 2019). Due to its excellent biocontrol effect, *Bacillus spp.* have been useful in the field of agricultural production. Research on *B. velezensis* is mainly focused on promoting animal and plant growth, antagonizing pathogens, inducing systemic resistance, identifying bacteriostatic substances and their gene clusters, and antagonistic mechanism (Gao et al., 2017; Cao et al., 2018; Chen et al., 2018). In the prevention and control of plant diseases, *B. velezensis* has showed good antagonistic effect against many plant pathogenic fungi and bacteria,

such as *Alternaria solani*, *Phytophthora capsici*, *Fusarium solani*, *Botrytis cinerea Pers*, *Fusarium oxysporum*, *Streptomyces galilaeus*, and *Rhizoctonia solani* (Ait Kaki et al., 2013; Kanjanamaneesathian et al., 2013; Lim et al., 2017). In animals, it has shown good inhibitory effect on common pathogens such as *E. coli*, *Salmonella enteritis*, *Campylobacter jejuni*, *Listeria monocytogenes*, *Aeromonas hydrophila*, *Streptococcus agalactis,* and *Vibrio parahaemolyticus* (Nannan et al., 2018; Yi et al., 2018). In this study, we observed that the fermentation broth of *B. velezensis* had good antibacterial effect, especially against *S. aureus*, with an inhibitory zone diameter of 32.16 ± 2.04 mm. Therefore, *B. velezensis* Ea73 is expected to be an important strain resource for the development of natural antibiotic products.

Fermentation broths do not only contain a small amount of metabolic active substances, but also a large number of impurities that affect the antimicrobial activity. The type and proportion of compounds in the culture medium affect the antimicrobial potency of the fermentation broth (Sanchez and Demain, 2002). Therefore, there is the need to investigate the ideal broth conditions that will yield the maximum antimicrobial activity.

TABLE 4 | Design and experimental results of Box–Behnken design (fermentation parameters).

Run	A	B (°C)	C (h)	Response (mm)
1	7	24	48	36.34
2	9	24	48	36.30
3	7	30	48	38.93
4	9	30	48	37.73
5	7	27	24	35.88
6	9	27	24	36.45
7	7	27	72	36.18
8	9	27	72	36.77
9	8	24	24	30.81
10	8	30	24	35.95
11	8	24	72	36.00
12	8	30	72	38.27
13	8	27	48	40.25
14	8	27	48	40.16
15	8	27	48	40.99

TABLE 5 | ANOVA results of the quadratic model (fermentation parameters).

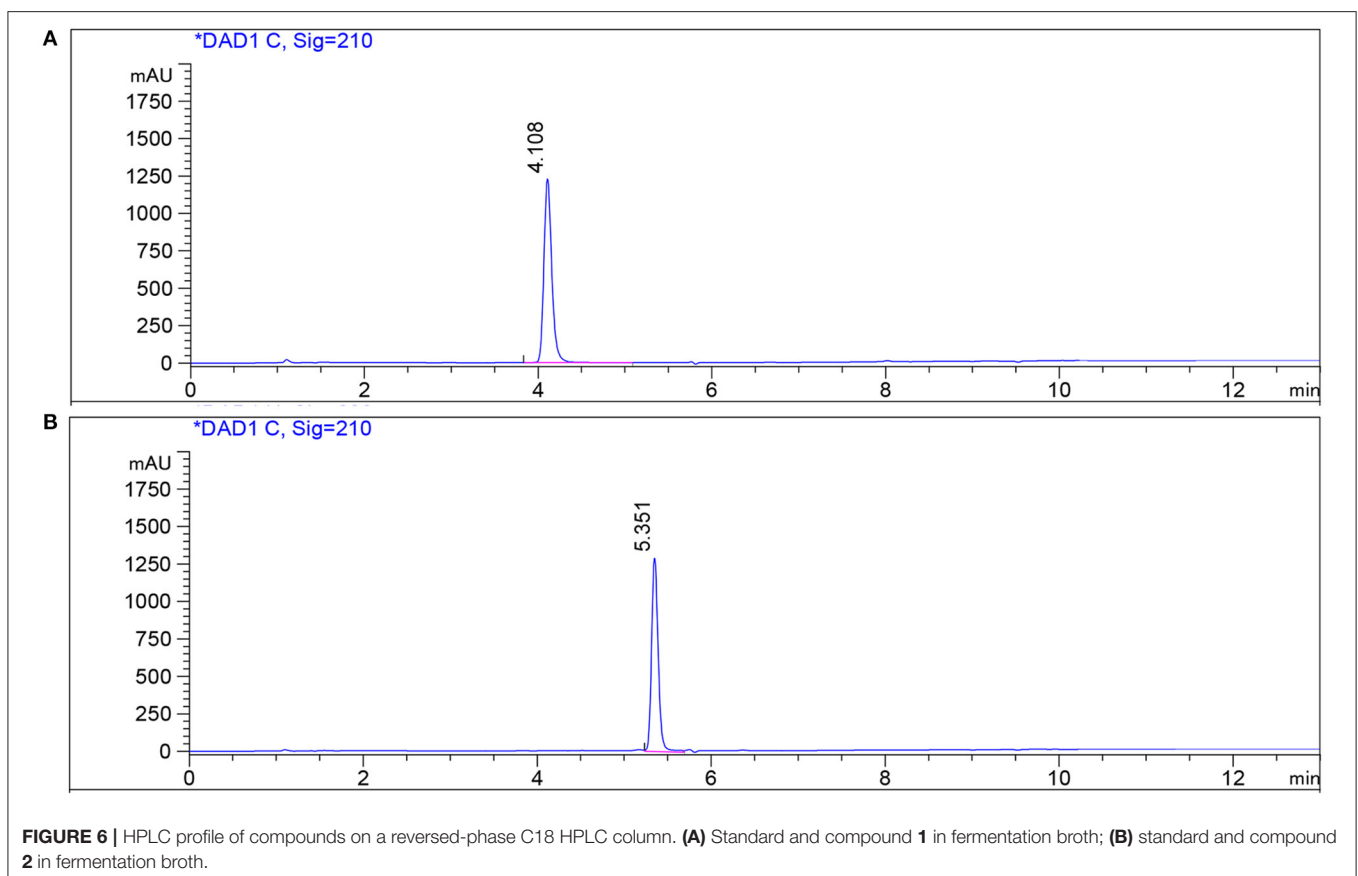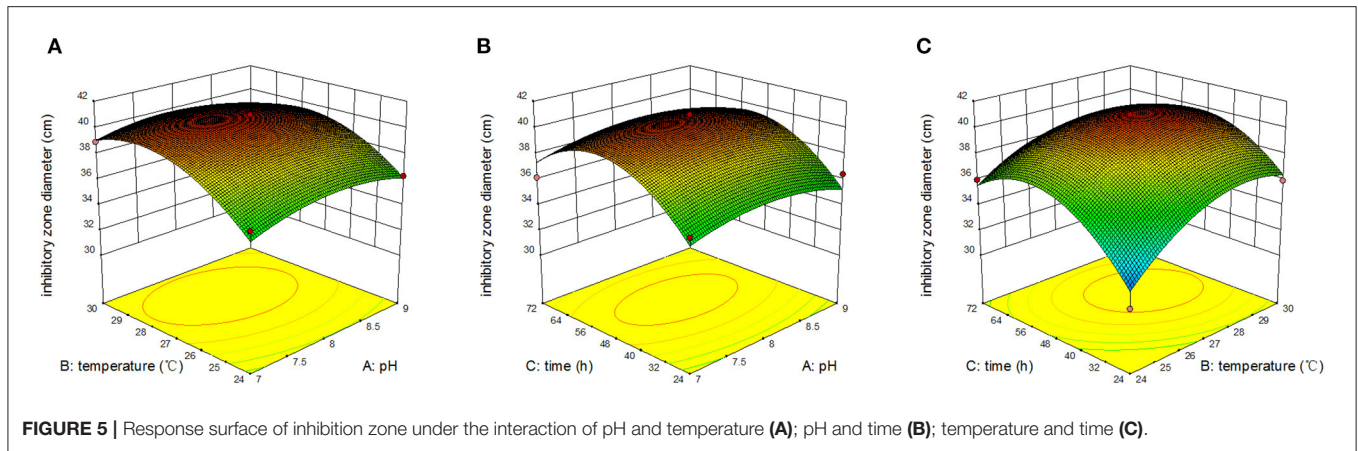| Source	Sum of squares	df	Mean square	F-Value	p-Value, Probability > F
Model	77.19	9	8.58	5.04	0.0448
A-pH	8.000E-004	1	8.000E-004	4.703E-004	0.9835
B-temperature	16.33	1	16.33	9.60	0.0269
C-time	8.26	1	8.26	4.86	0.0787
AB	0.34	1	0.34	0.20	0.6751
AC	1.000E-004	1	1.000E-004	5.879E-005	0.9942
BC	2.06	1	2.06	1.21	0.3214
A^2	3.99	1	3.99	2.35	0.1862
B^2	16.32	1	16.32	9.59	0.0269
C^2	35.65	1	35.65	20.95	0.0060
Residual	8.51	5	1.70		
Lack of fit	8.09	3	2.70	13.00	0.0723
Pure error	0.41	2	0.21		
Cor total	85.70	14			

In this study, taking the inhibitory activity of fermentation broth against *S. aureus* as an index, a single-factor test combined with response surface analysis was used to optimize the proportion of culture medium and fermentation conditions of *B. velezensis* Ea73. The results showed that the inhibitory activity of strain Ea73 was affected in the order of yeast extract > temperature > peptone > time > NaCl > pH. In addition, inhibitory activities were effective when the yeast extract in the media was 6.55 g/L, peptone was 6.61 g/L, NaCl was 20.00 g/L, initial pH was 7.95, temperature was 27.97°C, and harvest time was 51.04 h. At these media conditions, the inhibitory zone diameter of strain Ea73 against *S. aureus* reached the maximum (which was 40.76 mm). Therefore, compared to the inhibitory zone diameter produced by fermentation broth

before optimization, the antibacterial activity of strain Ea73 was significantly improved after optimization.

Studies have shown that *B. velezensis* has a remarkable ability to produce secondary metabolites with strong antimicrobial properties such as lipopeptides, surfactin, fengycin, and bacillomycin D, macrolactin, bacillaene, difficidin, or oxydifficidin; and peptides (Chen et al., 2015; Khalid et al., 2021b). However, the strain type, composition, and conditions of fermentation medium affect the yield and type of secondary antibacterial metabolites produced by various strains (Khan et al., 2017; Arokiyaraj et al., 2019). For example, Pournejati et al. (2019) optimized the fermentation conditions of *B. velezensis* RP137 and found that when rice starch and potassium nitrate were supplied to the strain RP137, it increased the production of aminoglycoside antibacterial metabolites. Khalid et al. (2021a) optimized the fermentation parameters (temperature, time, pH, and loaded liquid volume) for *B. velezensis* JTYP2 and found that all these parameters differently affected β-glucanase and protease production. The main antibacterial metabolites isolated by Nam and colleagues from *B. velezensis* NST6 was C15-bacillomycin D (Nam et al., 2021). Therefore, after optimizing the antibacterial activity of strain Ea73, we continued to isolate and purify its antibacterial metabolites.

The two antibacterial metabolites that were purified from the fermentation broth of *B. velezensis* Ea73 were identified as Cyclo (*L*-Pro-*L*-Val) and Cyclo (*L*-Leu-*L*-Pro) by NMR, IR, and HRMS. The above results were further confirmed by comparing the physical and spectral data of the two cyclic dipeptides (CDPs) with the values described in literatures. CDPs are formed by the internal cyclization of two amino acid amides, and a matrix of 2-diketo-piperazine or 2-dioxopiperazine (Saadouli et al., 2020). They are the simplest, naturally occurring cyclic forms of peptides, commonly biosynthesized by a large variety of living organisms and conserved in bacteria to humans (Bojarska et al., 2021).

Many studies have showed that CDPs possess a variety of biological properties such as antibacterial (Nishanth Kumar et al., 2012), antifungal (Ström et al., 2002), anticancer (Nishanth et al., 2014), neuroprotective (Bellezza et al., 2014), blood–brain barrier transporter (Teixidó et al., 2007), anticoagulation (Newman et al., 2003), anti-inflammatory (Minelli et al., 2012), and plant growth regulation activity (Ortiz-Castro et al., 2011). In this study, we observed that Cyclo (*L*-Pro-*L*-Val) and Cyclo (*L*-Leu-*L*-Pro) showed antibacterial effect on *S. aureus* and *E. coli*; however, it was not significant. This was similar to the results of Furtado et al. (2005), which isolated 7 CDPs [including Cyclo (*L*-Pro-*L*-Val) and Cyclo (*L*-Pro-*L*-Leu)] from *Aspergillus fumigatus* fermentation broth and reported that all the CDPs inhibited the growth of *S. aureus* and *Micrococcus luteus* at the concentration of 2.9 mmol/L. In other studies, the MIC value of Cyclo (*L*-Leu-*L*-Pro) against *L. monocytogenes* ATCC 19111 was found to be 512 μg/ml (Gowrishankar et al., 2016), whereas MIC value of Cyclo (Leu-Pro) on *P. aeruginosa* PAO1 was 250 μg/ml (Parasuraman et al., 2020). In contrast, Kaaniche et al. (2020) revealed that both Cyclo (Leu-Pro) and Cyclo (Val-Pro) demonstrated significant antibacterial activity against *Agrobacterium tumefaciens* ATCC
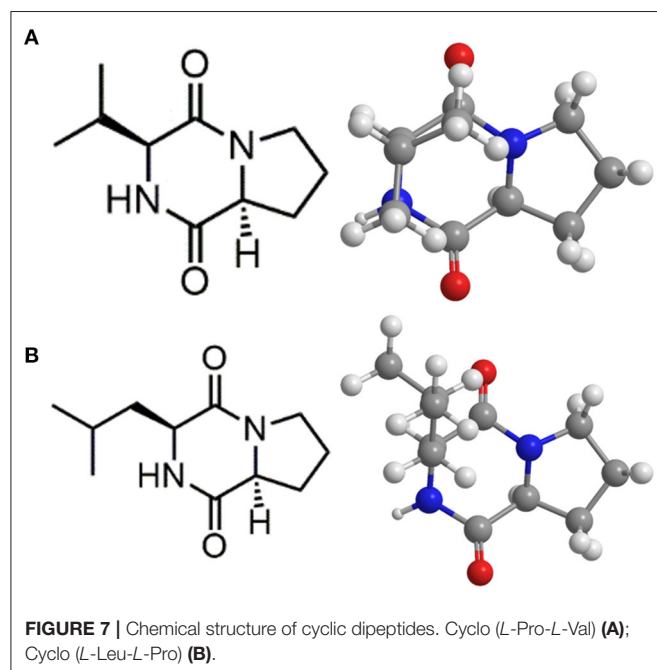
FIGURE 5 | Response surface of inhibition zone under the interaction of pH and temperature **(A)**; pH and time **(B)**; temperature and time **(C)**.

FIGURE 6 | HPLC profile of compounds on a reversed-phase C18 HPLC column. **(A)** Standard and compound **1** in fermentation broth; **(B)** standard and compound **2** in fermentation broth.

23308, *L. monocytogenes* ATCCC 19117, *S. aureus* ATCC 6538, and *Salmonella typhimurium* ATCC 14028, at MIC values of (10, 20, 20, 10) and (12, 20, 20, 10) μg/ml, respectively.

The differences in activity may be attributed to the absolute configuration. For example, a study by Kaaniche et al. (2020) showed that five CDPs [Cyclo (*D*-Phe-*D*-Pro), Cyclo (*D*-Leu-*D*-Pro), Cyclo (*D*-Pro-*D*-Val), Cyclo (*D*-Ile-*D*-Pro), and Cyclo (*D*-Phe-*trans*-4-OH-*D*-Pro)] with the *D*-configuration of the amino acid had different MIC values [Cyclo (*D*-Phe-*L*-Pro) had MIC value of 0.13 μg/ml, Cyclo (*D*-Phe-*D*-Pro) had MIC value of 0.03 μg/ml, and the diastereomer Cyclo (*L*-Phe-*D*-Pro) had MIC value of 0.10 μg/mL] against *Vibrio anguillarum*. Furthermore, comparing their stereoisomers, the authors pointed out that at least one *D*-amino acid was required for antibacterial activity. Although different combinations of *D*- and *L*-amino acids activate antibacterial activity, the DD-enantiomers have higher activity (Kaaniche et al., 2020). This was confirmed by Kumar et al. (2012), who reported that the MIC values of Cyclo (*L*-Leu-*L*-Pro) against *S. aureus* and *E. coli* were 32 and 250 μg/ml, respectively, whereas that of Cyclo (*D*-Pro-*L*-Leu) to the same

TABLE 6 | ^{1}H and ^{13}C NMR data for compounds **1** and **2** (CDCl$_3$, 500 MHz, δ in ppm).

Positions	Compound 1		Compound 2	
	$\delta^{C(ppm)}$	δ^H, Mult. (J in Hz)	$\delta^{C(ppm)}$	δ^H, Mult. (J in Hz)
1	170.08		170.08	
NH		6.07 (s, 1H)		5.77 (s, 1H)
2	60.40	3.95–3.90 (m, 1H)	59.00	4.02 (dd, J = 9.5, 3.7 Hz, 1H)
3	164.94		164.94	
4	45.15	3.67–3.59 (m, 1H)	45.53	3.65–3.51 (m, 2H)
		3.57–3.48 (m, 1H)		
5	28.54	2.07–1.99 (m, 2H)	28.14	2.10–1.98 (m, 2H)
6	22.38	2.40–2.33 (m, 1H)	22.76	2.17–2.10 (m, 1H)
		1.96–1.84 (m, 1H)		1.97–1.83 (m, 1H)
7	58.83	4.09–4.05 (m, 1H)	53.38	4.15–4.08 (m, 1H)
8	28.39	δ 2.69–2.56 (m, 1H)	24.75	2.40–2.30 (m, 1H)
9	19.23	1.06 (d, J = 7.3 Hz, 3H)	23.32	1.06 (d, J = 7.3 Hz, 3H)
10	16.07	0.90 (d, J = 6.8 Hz, 3H)	21.18	0.90 (d, J = 6.8 Hz, 3H)
11			38.64	1.79–1.66 (m, 1H)
				1.52 (ddd, J = 14.5, 9.6, 5.0 Hz, 1H)

FIGURE 7 | Chemical structure of cyclic dipeptides. Cyclo (*L*-Pro-*L*-Val) **(A)**; Cyclo (*L*-Leu-*L*-Pro) **(B)**.

bacteria were 64 and 32 μg/ml. These results indicated that, among the three enantiomers (*LL, DL,* and *DD*), the antibiotic activity of *DD*- enantiomers seems to be the highest, and the activity of *D*-amino acids is stronger than that of *L*-enantiomers. This confirms the report that *D*-amino acids are responsible for biofilm disassembly of *Bacillus subtilis* (Kolodkin-Gal et al.,

2010; Hochbaum et al., 2011). However, the relationship between enantiomers and activity was not fully confirmed in this study, hence it needs further studies.

A large number of studies have shown that CDPs also have synergistic antibacterial effect. A study by Kumar et al. (2012) reported the synergistic activity of Cyclo (*L*-Pro-*L*-Leu), Cyclo (*D*-Pro-*L*-Leu), and Cyclo (*D*-Pro-*L*-Tyr) against bacteria *in vitro*. The combination of CDPs and amphotericin B or clotrimazole also had synergistic effect against *Candida albicans in vitro* (Kumar et al., 2013). Rhee (2004) studied the synergistic antibacterial effect of two CDPs Cyclo (*L*-Leu-*L*-Pro) and Cyclo (*L*-Phe-*L*-Pro) *in vitro*. The results showed that the combination of the two drugs could effectively inhibit the growth of vancomycin-resistant enterococci with MIC value of 0.25–1 mg/L. In addition, it also showed a strong inhibitory effect on pathogenic bacteria such as *E. coli*, *S. aureus,* and *C. albicans* at MIC value of 0.25–0.5 mg/L. Combination therapy can be used to expand the antimicrobial spectrum to prevent the emergence of resistant organisms. Therefore, the synergistic activity of CDPs can be developed and utilized to eliminate pathogens.

There is more to the development and utilization of CDPs as we can focus on the molecular self-assembly properties of CDPs. CDPs contains a six-membered cyclolactam ring with two amide bonds, in which functional groups could be presented at a total of six locations and four positions controlled by stereochemistry (Borthwick, 2012; Borgman et al., 2019). The diverse functional properties and applications arise from the unique structural attributes of CDPs, conformational rigidity, strong intermolecular interactions, proteolytic stability, biological relevance, and biocompatibility (Balachandra et al., 2021). Rationally designed CDPs have been utilized for the development of unique materials such as low-molecular-weight gelators (Kleinsmann and Nachtsheim, 2013), AIEgenic systems (Balachandra and Govindaraju, 2020), antioxidant CDPs (Manchineella et al., 2017), and quantum-confined materials (Tao et al., 2018). CDPs are also scaffold for the syntheses of various complex natural products (González et al., 2012). Overall, the structural and functional diversity of CDPs exemplify its significance and utility across the domains of chemistry, biology, and materials science.

In this study, we successfully isolated and characterized *B. velezensis* Ea73 from *A. adenophora*. *B. velezensis* Ea73 showed a strong antibacterial activity and genetic stability against *E. coli*, *Salmonella*, *P. aeruginosa*, *K. pneumonia,* and *S. aureus*. We also found that the maximum antibacterial activity was observed when the concentrations of yeast extract, peptone, and NaCl in the culture media were 6.55, 6.61, and 20.00 g/L, respectively, and the initial pH, harvesting time, and temperature of the culture media were 7.95, 51.04 h, and 27.97°C, respectively. Under these conditions, the inhibitory zone diameter of Ea73 fermentation broth against *S. aureus* reached 40.76 mm. Furthermore, two antibacterial peptides, Cyclo (*L*-Pro-*L*-Val) and Cyclo (*L*-Leu-*L*-Pro), were successfully isolated from *B. velezensis* Ea73. These two CDPs had mild antibacterial activity against *S. aureus* and *E. coli*. Therefore, we stipulated that *A. adenophora* contains antibacterial endophytes with numerous antibacterial metabolites that may serve as alternative sources for the

development of natural antibiotics; however, further studies are still required to elucidate the complete mechanisms of action by confirming the efficacy of these two compounds through *in vivo* experiments.

DATA AVAILABILITY STATEMENT

The original contributions presented in the study are included in the article/**Supplementary Material**, further inquiries can be directed to the corresponding author/s.

AUTHOR CONTRIBUTIONS

ZR, LX, and SO: conceptualization, methodology, and software. ZR, LX, SO, JW, and YR: data collection, writing, and original draft preparation. SO, JW, XN, and YR: validation and investigation. ZR, XN, and YH: funding and supervision. All authors read and agreed to the published version of the manuscript.

SUPPLEMENTARY MATERIAL

The Supplementary Material for this article can be found online at: https://www.frontiersin.org/articles/10.3389/fmicb.2022.860009/full#supplementary-material

REFERENCES

Ait Kaki, A., Kacem Chaouche, N., Dehimat, L., Milet, A., Youcef-Ali, M., Ongena, M., et al. (2013). Biocontrol and plant growth promotion characterization of *Bacillus* species isolated from *Calendula officinalis* rhizosphere. *Indian J. Pathol. Microbiol.* 53, 447–452. doi: 10.1007/s12088-013-0395-y

Amin, D. H., Abdallah, N. A., Abolmaa Ty, A., Tolba, S., and Wellington, E. (2020). Microbiological and molecular insights on rare actinobacteria harboring bioactive prospective. *Bull. Natl. Res. Cent.* 44, 1–12. doi: 10.1186/s42269-019-0266-8

Arokiyaraj, S., Varghese, R., Ali Ahmed, B., Duraipandiyan, V., and Al-Dhabi, N. A. (2019). Optimizing the fermentation conditions and enhanced production of keratinase from *Bacillus cereus* isolated from halophilic environment. *Saudi J. Biol. Sci.* 26, 378–381. doi: 10.1016/j.sjbs.2018.10.011

Balachandra, C., and Govindaraju, T. (2020). Cyclic dipeptide-guided aggregation-induced emission of naphthalimide and its application for the detection of phenolic drugs. *J. Org. Chem.* 85, 1525–1536. doi: 10.1021/acs.joc.9b02580

Balachandra, C., Padhi, D., and Govindaraju, T. (2021). Cyclic dipeptide: a privileged molecular scaffold to dderive structural diversity and functional utility. *Chem. Med. Chem.* 16, 2558–2587. doi: 10.1002/cmdc.202100149

Bellezza, I., Peirce, M. J., and Minelli, A. (2014). Cyclic dipeptides: from bugs to brain. *Trends Mol. Med.* 20:551–558. doi: 10.1016/j.molmed.2014.08.003

Bojarska, J., Mieczkowski, A., Ziora, Z. M., Skwarczynski, M., Toth, I., Shalash, A. O., et al. (2021). Cyclic dipeptides: the biological and structural landscape with special focus on the anti-cancer proline-based scaffold. *Biomolecules* 11, 1515. doi: 10.3390/biom11101515

Borgman, P., Lopez, R. D., and Lane, A. L. (2019). Correction: the expanding spectrum of diketopiperazine natural product biosynthetic pathways containing cyclodipeptide synthases. *Org. Biomol. Chem.* 17, 3066. doi: 10.1039/C9OB90038A

Borthwick, A. D. (2012). 2,5-Diketopiperazines: synthesis, reactions, medicinal chemistry, and bioactive natural products. *Chem. Rev.* 112, 3641–3716. doi: 10.1021/cr200398y

Cao, Y., Pi, H., Chandrangsu, P., Li, Y., Wang, Y., Zhou, H., et al. (2018). Antagonism of two plant-growth promoting *Bacillus velezensis* isolates against *Ralstonia solanacearum* and *Fusarium oxysporum*. *Sci. Rep.* 8, 4360. doi: 10.1038/s41598-018-22782-z

Chen, L., Heng, J., Qin, S., and Bian, K. (2018). A comprehensive understanding of the biocontrol potential of *Bacillus velezensis* LM2303 against *Fusarium* head blight. *PLoS ONE* 13, e0198560. doi: 10.1371/journal.pone.0198560

Chen, W. C., Juang, R. S., and Wei, Y. H. (2015). Applications of a lipopeptide biosurfactant, surfactin, produced by microorganisms. *Biochem. Eng. J.* 103, 158–169. doi: 10.1016/j.bej.2015.07.009

Chernov, V. M., Chernova, O. A., Mouzykantov, A. A., Lopukhov, L. L., and Aminov, R. I. (2019). Omics of antimicrobials and antimicrobial resistance. *Expert Opin. Drug Discov.* 14, 455–468. doi: 10.1080/17460441.2019.1588880

Cui, Y., Okyere, S. K., Gao, P., Wen, J., Cao, S., Wang, Y., et al. (2021). *Ageratina adenophora* disrupts the intestinal structure and immune barrier integrity in rats. *Toxins* 13, 651. doi: 10.3390/toxins13090651

Dereeper, A., Audic, S., Claverie, J. M., and Blanc, G. (2010). BLAST-EXPLORER helps you building datasets for phylogenetic analysis. *BMC Evol. Biol.* 10, 8. doi: 10.1186/1471-2148-10-8

Ding, Y., Li, Y., Li, Z., Zhang, J., Lu, C., Wang, H., et al. (2016). Alteramide B is a microtubule antagonist of inhibiting *Candida albicans*. *Biochim. Biophys. Acta Bioenerg.* 1860, 2097–2106. doi: 10.1016/j.bbagen.2016.06.025

du Toit, E. A., and Rautenbach, M. (2000). A sensitive standardised micro-gel well diffusion assay for the determination of antimicrobial activity. *J. Microbiol. Methods* 42, 159–165. doi: 10.1016/S0167-7012(00)00184-6

Fu, J., Hu, L., Shi, Z., Sun, W., Yue, D., Wang, Y., et al. (2021). Two metabolites isolated from endophytic fungus *Coniochaeta* sp. F-8 in *Ageratina adenophora* exhibit antioxidative activity and cytotoxicity. *Nat. Prod. Res.* 35, 2840–2848. doi: 10.1080/14786419.2019.1675060

Furtado, N., Pupo, M. T., Ivone, C., Campo, V. L., Duarte, M., and Bastos, J. K. (2005). Diketopiperazines produced by an *Aspergillus fumigatus* Brazilian strain. *J. Braz. Chem. Soc.* 16, 1448–1453. doi: 10.1590/S0103-50532005000800026

Gao, X. Y., Liu, Y., Miao, L. L., Li, E. W., Sun, G. X., Liu, Y., et al. (2017). Characterization and mechanism of anti-*Aeromonas salmonicida* activity of a marine probiotic strain, *Bacillus velezensis* V4. *Appl. Microbiol. Biotechnol.* 101, 3759–3768. doi: 10.1007/s00253-017-8095-x

González, J. F., Ortín, I., de la Cuesta, E., and Menéndez, J. C. (2012). Privileged scaffolds in synthesis: 2,5-piperazinediones as templates for the preparation of structurally diverse heterocycles. *Chem. Soc. Rev.* 41, 6902–6915. doi: 10.1039/c2cs35158g

Gowrishankar, S., Sivaranjani, M., Kamaladevi, A., Ravi, A. V., Balamurugan, K., and Karutha Pandian, S. (2016). Cyclic dipeptide cyclo(*l*-leucyl-*l*-prolyl) from marine *Bacillus amyloliquefaciens* mitigates biofilm formation and virulence in *Listeria monocytogenes*. *Pathog. Dis.* 74, ftw017. doi: 10.1093/femspd/ftw017

Hallmann, J. A., Quadt-Hallmann, A., Mahaffee, W. F., and Kloepper, J. W. (2011). Bacterial endophytes in agricultural crops. *Can. J. Microbiol.* 43, 895–914. doi: 10.1139/m97-131

He, Y., Mo, Q., Luo, B., Qiao, Y., Xu, R., Zuo, Z., et al. (2016). Induction of apoptosis and autophagy via mitochondria- and PI3K/Akt/mTOR-mediated pathways by *E. adenophorum* in hepatocytes of saanen goat. *Oncotarget* 7, 54537–54548. doi: 10.18632/oncotarget.10402

Hochbaum, A. I., Kolodkin-Gal, I., Foulston, L., Kolter, R., Aizenberg, J., and Losick, R. (2011). Inhibitory effects of *D*-amino acids on *Staphylococcus aureus* biofilm development. *J. Bacteriol. Res.* 193, 5616–5622. doi: 10.1128/JB.05534-11

Jeong, M. H., Lee, Y. S., Cho, J. Y., Ahn, Y. S., Moon, J. H., Hyun, H. N., et al. (2017). Isolation and characterization of metabolites from *Bacillus licheniformis* MH48 with antifungal activity against plant pathogens. *Microb. Pathog.* 110, 645–653. doi: 10.1016/j.micpath.2017.07.027

Jiang, H. (2010). *Diversity of Endophytic Fungi in the Leaves of Invasive Plant Eupatorium Adenophorum Spreng*. (Dissertation/Doctoral thesis), Yunnan University, Kunming (China).

Jin, Y., Hou, L., Zhang, M., Tian, Z., Cao, A., and Xie, X. (2014). Antiviral activity of *Eupatorium adenophorum* leaf extract against tobacco mosaic virus. *Crop Prot.* 60, 28–33. doi: 10.1016/j.cropro.2014.02.008

Kaaniche, F., Hamed, A., Elleuch, L., Chakchouk-Mtibaa, A., Smaoui, S., Karray-Rebai, I., et al. (2020). Purification and characterization of seven bioactive compounds from the newly isolated *Streptomyces cavourensis* TN638 strain via solid-state fermentation. *Microb. Pathog.* 142, 104106. doi: 10.1016/j.micpath.2020.104106

Kang, Y. (2010). *Basic Research on Eupatorium Adenophorum and Its Root Endophytic Fungi in Heavy Metal Mining Area*. (Dissertation/Doctoral thesis), Yunnan University, Kunming (China).

Kanjanamaneesathian, M., Wiwattanapatapee, R., Rotniam, W., Pengnoo, A., and Tanmala, V. (2013). Application of a suspension concentrate formulation of *Bacillus velezensis* to control root rot of hydroponically-grown vegetables. *N. Z. Plant Prot.* 66, 229-234. doi: 10.30843/nzpp.2013.66.5556

Khalid, A., Ye, M., Wei, C., Dai, B., Yang, R., Huang, S., et al. (2021a). Production of β-glucanase and protease from *Bacillus velezensis* strain isolated from the manure of piglets. *Prep. Biochem. Biotechnol.* 51, 497–510. doi: 10.1080/10826068.2020.1833344

Khalid, F., Khalid, A., Fu, Y., Hu, Q., Zheng, Y., Khan, S., et al. (2021b). Potential of *Bacillus velezensis* as a probiotic in animal feed: a review. *J. Microbiol.* 59, 627–633. doi: 10.1007/s12275-021-1161-1

Khan, M. N., Lin, H., Li, M., Wang, J., Mirani, Z. A., Khan, S. I., et al. (2017). Identification and growth optimization of a Marine *Bacillus* DK1-SA11 having potential of producing broad spectrum antimicrobial compounds. *Pak. J. Pharm. Sci.* 30, 839–853.

Kleinsmann, A. J., and Nachtsheim, B. J. (2013). Phenylalanine-containing cyclic dipeptides–the lowest molecular weight hydrogelators based on unmodified proteinogenic amino acids. *Chem. Commun.* 49, 7818–7820. doi: 10.1039/c3cc44110e

Kolodkin-Gal, I., Romero, D., Cao, S., Clardy, J., Kolter, R., and Losick, R. (2010). *D*-amino acids trigger biofilm disassembly. *Science* 328, 627–629. doi: 10.1126/science.1188628

Kong, Y., Kong, J., Wang, D., Huang, H., Geng, K., Wang, Y., et al. (2017). Effect of *Ageratina adenophora* invasion on the composition and diversity of soil microbiome. *J. Gen. Appl. Microbiol.* 63, 114–121. doi: 10.2323/jgam.2016.08.002

Kumar, S. N., Nambisan, B., Mohandas, C., and Sundaresan, A. (2013). *In vitro* synergistic activity of diketopiperazines alone and in combination with amphotericin B or clotrimazole against *Candida albicans*. *Folia Microbiol.* 58, 475–482. doi: 10.1007/s12223-013-0234-x

Kumar, S. N., Siji, J. V., Nambisan, B., and Mohandas, C. (2012). Activity and synergistic antimicrobial activity between diketopiperazines against bacteria *in vitro*. *Appl. Biochem. Biotechnol.* 168, 2285–2296. doi: 10.1007/s12010-012-9937-8

Liang, X. H., Cai, Y. J., Liao, X. R., Wu, K., Wang, L., Zhang, D. B., et al. (2009). Isolation and identification of a new hypocrellin A-producing strain *Shiraia* sp. SUPER-H168. *Microbiol. Res.* 164, 9–17. doi: 10.1016/j.micres.2008.08.004

Liao, F., Hu, Y., Wu, L., Tan, H., Mo, Q., Luo, B., et al. (2014). Antitumor activity *in vitro* by 9-Oxo-10,11-dehydroageraphorone extracted from *Eupatorium adenophorum*. *Asian J. Chem.* 26, 7321–7323.doi: 10.14233/ajchem.2014.16696

Lim, S. M., Yoon, M. Y., Choi, G. J., Choi, Y. H., Jang, K. S., Shin, T. S., et al. (2017). Diffusible and volatile antifungal compounds produced by an antagonistic *Bacillus velezensis* G341 against various phytopathogenic fungi. *Plant Pathol.* 33, 488–498. doi: 10.5423/PPJ.OA.04.2017.0073

Manchineella, S., Voshavar, C., and Govindaraju, T. (2017). Radical-scavenging antioxidant cyclic dipeptides and silk fibroin biomaterials. *Eur. J. Org. Chem.* 30, 4363–4369. doi: 10.1002/ejoc.201700597

Mcgeoch, M. A., Butchart, S., Spear, D., Marais, E., and Hoffmann, M. (2010). Global indicators of biological invasion: species numbers, biodiversity impact and policy responses. *Divers. Distrib* 16, 95–108. doi: 10.1111/j.1472-4642.2009.00633.x

Minelli, A., Grottelli, S., Mierla, A., Pinnen, F., Cacciatore, I., and Bellezza, I. (2012). Cyclo(His-Pro) exerts anti-inflammatory effects by modulating NF-κB and Nrf2 signalling. *Int. J. Biochem. Cell Biol.* 44, 525–535. doi: 10.1016/j.biocel.2011.12.006

Nam, J., Alam, S. T., Kang, K., Choi, J., and Seo, M. H. (2021). Anti-staphylococcal activity of a cyclic lipopeptide, C15 -bacillomycin D, produced by *Bacillus velezensis* NST6. *J. Appl. Microbiol.* 131, 93–104. doi: 10.1111/jam.14936

Nannan, C., Gillis, A., Caulier, S., and Mahillon, J. (2018). Complete genome sequence of *Bacillus velezensis* CN026 exhibiting antagonistic activity against gram-negative foodborne pathogens. *Genome Announc.* 6, e01543–17. doi: 10.1128/genomeA.01543-17

Newman, D. J., Cragg, G. M., and Snader, K. M. (2003). Natural products as sources of new drugs over the period 1981-2002. *J. Nat. Prod.* 66, 1022–1037. doi: 10.1021/np030096l

Nishanth Kumar, S., Mohandas, C., Siji, J. V., Rajasekharan, K. N., and Nambisan, B. (2012). Identification of antimicrobial compound, diketopiperazines, from a *Bacillus* sp. N strain associated with a rhabditid entomopathogenic nematode against major plant pathogenic fungi. *J. Appl. Microbiol.* 113, 914–924. doi: 10.1111/j.1365-2672.2012.05385.x

Nishanth, S. K., Nambisan, B., and Dileep, C. (2014). Three bioactive cyclic dipeptides from the *Bacillus* sp. N strain associated with entomopathogenic nematode. *Peptides* 53, 59–69. doi: 10.1016/j.peptides.2013.11.017

Okyere, S.K., Wen J., Cui, Y., Xie, L., Gao, P., Zhang, M., et al. (2022). *Bacillus toyonensis* SAU-19 and SAU-20 isolated from *Ageratina adenophora* alleviates the intestinal structure and integrity damage associated with gut dysbiosis in mice fed high fat diet. *Front. Microbiol.* 13, 820236. doi: 10.3389/fmicb.2022.820236

Okyere, S. K., Mo, Q., Pei, G., Ren, Z., Deng, J., and Hu, Y. (2020). Euptox A induces G0 /GI arrest and apoptosis of hepatocyte via ROS, mitochondrial dysfunction and caspases-dependent pathways *in vivo*. *J. Toxicol. Sci.* 45, 661–671. doi: 10.2131/jts.45.661

Okyere, S. K., Wen, J., Cui, Y., Xie, L., Gao, P., Wang, J., et al. (2021a). Toxic mechanisms and pharmacological properties of Euptox A, a toxic monomer from *A. adenophora*. *Fitoterapia* 155, 105032. doi: 10.1016/j.fitote.2021.105032

Okyere, S. K., Xie, L., Wen, J., Ran, Y., Ren, Z., Deng, J., et al. (2021b). *Bacillus toyonensis* SAU-19 ameliorates hepatic insulin resistance in high-fat diet/streptozocin-induced diabetic mice. *Nutrients* 13, 4512. doi: 10.3390/nu13124512

Ortiz-Castro, R., Díaz-Pérez, C., Martínez-Trujillo, M., del Río, R. E., Campos-García, J., and López-Bucio, J. (2011). Transkingdom signaling based on bacterial cyclodipeptides with auxin activity in plants. *Proc. Natl. Acad. Sci. U.S.A.* 108, 7253–7258. doi: 10.1073/pnas.1006740108

Parasuraman, P., Devadatha, B., Sarma, V. V., Ranganathan, S., Ampasala, D. R., Reddy, D., et al. (2020). Inhibition of microbial quorum sensing mediated virulence factors by *Pestalotiopsis sydowiana*. *J. Microbiol. Biotechnol.* 30, 571–582. doi: 10.4014/jmb.1907.07030

Pedras, M. S., Yu, Y., Liu, J., and Tandron-Moya, Y. A. (2005). Metabolites produced by the phytopathogenic fungus *Rhizoctonia solani*: isolation, chemical structure determination, syntheses and bioactivity. *J. Biosci.* 60, 717–722. doi: 10.1515/znc-2005-9-1010

Pournejati, R., Gust, R., and Karbalaei-Heidari, H. R. (2019). An aminoglycoside antibacterial substance, S-137-R, produced by newly isolated *Bacillus velezensis* strain RP137 from the Persian Gulf. *Curr. Microbiol.* 76, 1028–1037. doi: 10.1007/s00284-019-01715-7

Rabbee, M. F., Ali, M. S., Choi, J., Hwang, B. S., Jeong, S. C., and Baek, K. H. (2019). *Bacillus velezensis:* a valuable member of bioactive molecules within plant microbiomes. *Molecules* 24, 1046. doi: 10.3390/molecules24061046

Ren, Z., Gao, P., Okyere, S. K., Cui, Y., Wen, J., Jing, B., et al. (2021a). *Ageratina adenophora* inhibits spleen immune function in rats via the loss of the FRC network and Th1-Th2 cell ratio elevation. *Toxins* 13, 309. doi: 10.3390/toxins13050309

Ren, Z., Okyere, S. K., Wen, J., Xie, L., Cui, Y., Wang, S., et al. (2021b). An overview: the toxicity of *Ageratina adenophora* on animals and its possible interventions. *Int. J. Mol. Sci.* 22, 11581. doi: 10.3390/ijms222111581

Rhee, K. H. (2004). Cyclic dipeptides exhibit synergistic, broad spectrum antimicrobial effects and have anti-mutagenic properties. *Int. J. Antimicrob. Agents* 24, 423–427. doi: 10.1016/j.ijantimicag.2004.05.005

Saadouli, I., Zendah El Euch, I., Trabelsi, E., Mosbah, A., Redissi, A., Ferjani, R., et al. (2020). Isolation, characterization and chemical synthesis of large spectrum antimicrobial cyclic dipeptide (l-leu-l-pro) from *Streptomyces misionensis* V16R3Y1 bacteria extracts. A novel ^{1}H NMR metabolomic approach. *Antibiotics* 9, 270. doi: 10.3390/antibiotics9050270

Samuel, L., Lalrotluanga, M. R. B., Gurusubramanian, G., and Senthilkumar, N. (2014). Larvicidal activity of *Ipomoea cairica* (L.) sweet and *Ageratina adenophora* (Spreng.) King & H. Rob. plant extracts against arboviral and filarial vector, Culex quinquefasciatus say (diptera: culicidae). *Exp. Parasitol.* 141, 112–121. doi: 10.1016/j.exppara.2014.03.020

Sanchez, S., and Demain, A. L. (2002). Metabolic regulation of fermentation processes. *Enzyme Microb. Technol.* 31, 895–906. doi: 10.1016/S0141-0229(02)00172-2

Strobel, G., Daisy, B., Castillo, U., and Harper, J. (2004). Natural products from endophytic microorganisms. *J. Nat. Prod.* 67, 257–268. doi: 10.1021/np030397v

Ström, K., Sjögren, J., Broberg, A., and Schnürer, J. (2002). *Lactobacillus plantarum* MiLAB 393 produces the antifungal cyclic dipeptides cyclo(*L*-Phe-*L*-Pro) and cyclo(*L*-Phe-trans-4-OH-*L*-Pro) and 3-phenyllactic acid. *Appl. Environ. Microbiol.* 68, 4322–4327. doi: 10.1128/AEM.68.9.4322-4327.2002

Sun, X. H., Zhu, K. X., and Zhou, H. M. (2009). Optimization of a novel backward extraction of defatted wheat germ protein from reverse micelles. *Innov. Food Sci. Emerg. Technol.* 10, 328–333. doi: 10.1016/j.ifset.2009.01.006

Tanapichatsakul, C., Khruengsai, S., Monggoot, S., and Pripdeevech, P. (2019). Production of eugenol from fungal endophytes *Neopestalotiopsis* sp. and *Diaporthe* sp. isolated from *Cinnamomum loureiroi* leaves. *PeerJ* 7, e6427. doi: 10.7717/peerj.6427

Tanapichatsakul, C., Monggoot, S., Gentekaki, E., and Pripdeevech, P. (2018). Antibacterial and antioxidant metabolites of *Diaporthe* spp. isolated from flowers of *Melodorum fruticosum*. *Curr. Microbiol.* 75, 476–483. doi: 10.1007/s00284-017-1405-9

Tao, K., Fan, Z., Sun, L., Makam, P., Tian, Z., Ruegsegger, M., et al. (2018). Quantum confined peptide assemblies with tunable visible to near-infrared spectral range. *Nat. Commun.* 9, 3217. doi: 10.1038/s41467-018-05568-9

Teixidó, M., Zurita, E., Malakoutikhah, M., Tarragó, T., and Giralt, E. (2007). Diketopiperazines as a tool for the study of transport across the blood-brain barrier (BBB) and their potential use as BBB-shuttles. *J. Am. Chem. Soc.* 129, 11802–11813. doi: 10.1021/ja073522o

Tosi, M., Gaiero, J., Linton, N., Mafa-Attoye, T., Castillo, A., and Dunfield, K. (2021). Bacterial endophytes: diversity, functional importance, and potential for manipulation. *Rhizosphere Biol. Interact. Betw. Microb. Plants* 1, 1–49. doi: 10.1007/978-981-15-6125-2_1

Tripathi, Y. C., Saini, N., Anjum, N., and Verma, P. (2018). A review of ethnomedicinal, phytochemical, pharmacological and toxicological aspects of *Eupatorium adenophorum* Spreng. *Asian J. Biomed. Pharm. Sci.* 8, 25–35. doi: 10.13140/RG.2.2.25513.44642

Trivedi, P., Leach, J. E., Tringe, S. G., Sa, T., and Singh, B. K. (2020). Plant-microbiome interactions: from community assembly to plant health. *Nat. Rev. Microbiol.* 18, 607–621. doi: 10.1038/s41579-020-0412-1

Wan, F., Liu, W., Guo, J., Qiang, S., Li, B., Wang, J., et al. (2010). Invasive mechanism and control strategy of *Ageratina adenophora* (Sprengel). *Sci. China Life Sci.* 53, 1291–1298. doi: 10.1007/s11427-010-4080-7

Wen, J., Okyere, S. K., Wang, S., Wang, J., Xie, L., Ran, Y., et al. (2022). Endophytic fungi: an effective alternative source of plant-derived bioactive compounds for pharmacological studies. *J. Fungi* 8, 205. doi: 10.3390/jof8020205

Yao, B., Li, M., Sun, Y., Xiao, P., Jing, J., and Li, Q. (2019). Study on the inhibitory effect of *Eupatorium adenophorum* on plant pathogens. *Anhui Agric. Sci. Bull.* 25, 3.

Yi, Y., Zhang, Z., Zhao, F., Liu, H., Yu, L., Zha, J., et al. (2018). Probiotic potential of *Bacillus velezensis* JW: antimicrobial activity against fish pathogenic bacteria and immune enhancement effects on *Carassius auratus*. *Fish Shellfish Immunol.* 78, 322–330. doi: 10.1016/j.fsi.2018.04.055

Zhang, M., Liu, W. X., Zheng, M. F., Xu, Q. L., Wan, F. H., Wang, J., et al. (2013). Bioactive quinic acid derivatives from *Ageratina adenophora*. *Molecules* 18, 14096–14104. doi: 10.3390/molecules181114096